Loss-of-function mutations in the EGF-CFC gene *CFC1* are associated with human left-right laterality defects

Richard N. Bamford[1], Erich Roessler[1]*, Rebecca D. Burdine[2]*, Umay Şaplakoğlu[3]*, June dela Cruz[1], Miranda Splitt[4], Jeffrey Towbin[5], Peter Bowers[6], Bruno Marino[7], Alexander F. Schier[2], Michael M. Shen[3], Maximilian Muenke[1] & Brett Casey[8]

*These authors contributed equally to this work.

All vertebrates display a characteristic asymmetry of internal organs with the cardiac apex, stomach and spleen towards the left, and the liver and gall bladder on the right[1–3]. Left-right (L-R) axis abnormalities or laterality defects are common in humans (1 in 8,500 live births). Several genes (such as *Nodal*, *Ebaf* and *Pitx2*) have been implicated in L-R organ positioning in model organisms[2–4]. In humans, relatively few genes have been associated with a small percentage of human *situs* defects. These include *ZIC3* (ref. 5), *LEFTB* (formerly *LEFTY2*; ref. 6) and *ACVR2B* (encoding activin receptor IIB; ref. 7). The EGF-CFC genes[8], mouse *Cfc1* (encoding the Cryptic protein; ref. 9) and zebrafish *one-eyed pinhead* (*oep*; refs 10,11) are essential for the establishment of the L-R axis[12,13]. EGF-CFC proteins act as co-factors for Nodal-related signals[11], which have also been implicated in L-R axis development[4]. Here we identify loss-of-function mutations in human *CFC1* (encoding the CRYPTIC protein) in patients with heterotaxic phenotypes (randomized organ positioning). The mutant proteins have aberrant cellular localization in transfected cells and are functionally defective in a zebrafish *oep*-mutant rescue assay. Our findings indicate that the essential role of EGF-CFC genes and Nodal signalling in left-right axis formation is conserved from fish to humans. Moreover, our results support a role for environmental and/or genetic modifiers in determining the ultimate phenotype in humans.

To determine whether mutations in *CFC1* cause laterality defects, we compiled the full-length *CFC1* cDNA sequence on the basis of two EST clones (AA018899, AA862263) isolated from a human fetal brain library and 5′-RACE results using fetal brain total RNA. The cDNA clones identified an ORF of 223 amino acids and 5′ and 3′ UTRs of 391 bp and 97 bp, respectively. As with other EGF-CFC family members, *CFC1* is encoded by six exons with similar exon/intron spacing to *Cfc1* (Fig. 1*a*). CRYPTIC has a functional signal peptide (confirmed by *in vitro* translation/translocation

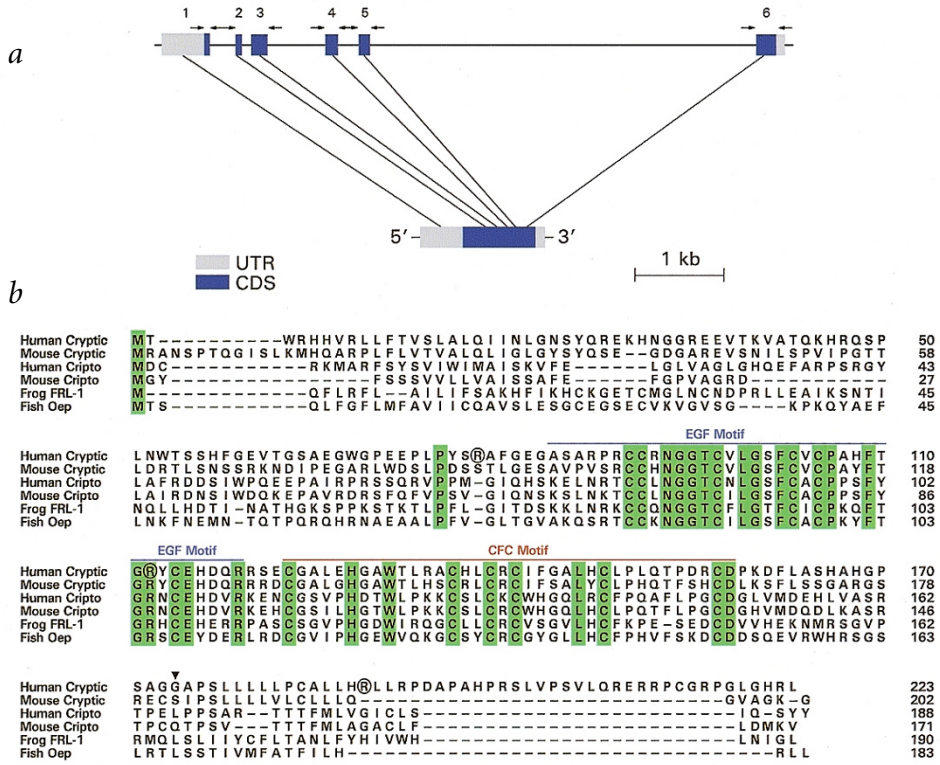

Fig. 1 Genomic structure and sequence alignment of *CFC1*. ***a***, A representative diagram of the six exons of the coding region (in blue) of *CFC1* is shown with the relative positions of the primers used in mutational analysis. A sequence alignment of the CRYPTIC protein is shown (***b***) with the positions of the missense mutations circled and the functional domains indicated by a solid blue line (EGF-Motif) or a solid red line (CFC-Motif). above the alignment. Invariant residues are boxed in green. The positions of missense mutations are indicated by circles. The position of the G174del1 mutation is marked by the inverted triangle. The predicted amino acid extension of G174del1 consists of the sequence RPACYSCCPA HSCTASCARMRPRTLGPWSLPSSSGSGA PAEGRDLGIAFNFLCCK.

[1]*Medical Genetics Branch, National Human Genome Research Institute, National Institutes of Health, Bethesda, Maryland, USA.* [2]*Developmental Genetics Program, Skirball Institute of Biomolecular Medicine, Department of Cell Biology, New York University School of Medicine, New York, New York, USA.* [3]*Center for Advanced Biotechnology and Medicine and Department of Pediatrics, UMDNJ-Robert Wood Johnson Medical School, Piscataway, New Jersey, USA.* [4]*Department of Human Genetics, University of Newcastle upon Tyne, Newcastle upon Tyne, UK.* [5]*Department of Pediatrics, Baylor College of Medicine, Houston, Texas, USA.* [6]*Department of Pediatrics, Yale University School of Medicine, New Haven, Connecticut, USA.* [7]*Department of Cardiology, Bambino Gesu' Children's Hospital, Rome, Italy.* [8]*Department of Pathology, Baylor College of Medicine, Houston, Texas, USA. Correspondence should be addressed to M.M. (e-mail: muenke@nih.gov).*

Table 1 • Clinical and molecular findings in patients with laterality defects

Patient	*CFC1* mutation	Laterality defects	Midline defects	Other clinical findings
1	334C→T R112C	CCA, R-sided stomach, intestinal malrotation	absent corpus callosum, myelocele	microcephaly
2	552delC G174del1	dextrocardia, TGA, L-isomerism of lungs, L-sided stomach, transverse liver, polysplenia, intestinal malrotation		
3	552delC G174del1 NODAL mutation	dextrocardia, TGA, R-isomerism of lungs, R artium, bilateral superior vena cava, R-sided stomach, asplenia		
4	562C→T R189C	CCA with L-atrial isomerism, VSD, polyspenia		
5	232C→T R78W	CCA, dextrocardia, DORV, PA, complete AV canal, TAPVR, PDA, R-sided aortic arch, R-isomerism of lungs, intestinal malrotation, asplenia		
6	232C→T R78W	HLHS, L-atrial isomerism, dysplasia of mitral valve & L ventricular outflow tract, R-isomerism of lungs, R-sided stomach, extrahepatic biliary atresia, polysplenia		
7	232C→T R78W	dextrocardia, TGA, common atrium, VSD, PA		
8	232C→T R78W	dextrocardia, ASD, VSD, PDA, hypoplastic aortic arch, central liver	omphalocele	14 ribs, absent ascending colon,appendix and transverse colon
9	232C→T R78W	membranous VSD	alobar HPE, cyclopia, single umbilical artery	13 ribs, limb and genitourinary anomalies

R, right; L, left; CCA, complex cardiac anomalies; VSD, ventricular septal defect; ASD, atrial septal defect; PDA, patent ductus arteriosus; DORV, double outlet right ventricle; TAPVR, total anomalous pulmonary venous return; PA, pulmonary atresia; TGA, transposition of great arteries; AV, atrio-ventricular; HLHS, hypoplastic left heart syndrome; HPE, holoprosencephaly.

studies; data not shown), a hydrophobic carboxy terminus required for membrane-association, and conserved EGF and CFC domains (Fig. 1*b*). The EGF-CFC regions of mouse and human CRYPTIC are 76% identical and 89% similar at the amino acid level, but the overall homology of these molecules is only 55% identical and approximately 70% similar. This low homology between mouse and human CRYPTIC is not unprecedented, as a similar divergence has been observed between mouse and human CRIPTO, another EGF-CFC family member[8]. Compared with mouse Cryptic, the coding sequence of CRYPTIC is extended by an additional 29 amino acids at the C terminus[14]. The significance of this difference is unknown.

For mutation detection in *CFC1*, we designed primers for SSCP in the flanking introns and/or UTRs of the exons (Fig. 1*a*). We screened 144 genomic DNAs representing unrelated sporadic and familial cases of L-R axis abnormalities, and sequenced amplicons demonstrating SSCP shifts. Similarly, 80 holoprosencephaly probands and an additional 27 individuals with right pulmonary isomerism were also studied. We identified 4 unique nucleotide changes in the laterality patient group that were not represented in over 200 normal control chromosomes. A heterozygous 334C→T transition corresponding to R112C in the EGF domain of exon 4 was present in patient 1 with sporadic L-R axis abnormalities (Table 1). This arginine residue is conserved in all EGF-CFC proteins (Fig. 1*b*). The same sequence change was inherited from a phenotypically normal parent, suggesting incomplete penetrance. In two unrelated sporadic patients (Table 1, patients 2 and 3), a heterozygous single-nucleotide deletion (522delC) corresponding to G174del1 was detected at the beginning of the membrane-associating domain

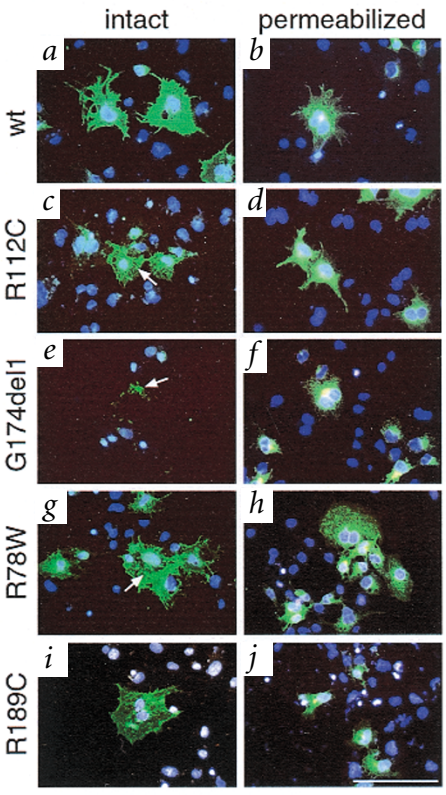

Fig. 2 Cellular localization of wild-type and variant CRYPTIC proteins in transfected COS cells. Immunofluorescence detection is shown of epitope-tagged CRYPTIC protein in intact (***a***,***c***,***e***,***g***,***i***) and detergent-permeabilized (***b***,***d***,***f***,***h***,***j***) cells, transfected with the indicated HA-tagged constructs. Note that the G174del1 mutant protein is absent from the cell surface (*e*), and may instead be partially associated with extracellular matrix (arrow). Additionally, the presence of G174del in permeabilized cells (*f*) indicates that its absence from the cell surface is not the result of rapid intracellular degradation. The R112C and R78W mutants are localized to the cell surface, but display prominent clustering of staining (arrows in *c*,*g*) that is not found in wild-type (*a*) or R189C (*i*) proteins. Scale bar for all panels, 100 μm (*j*).

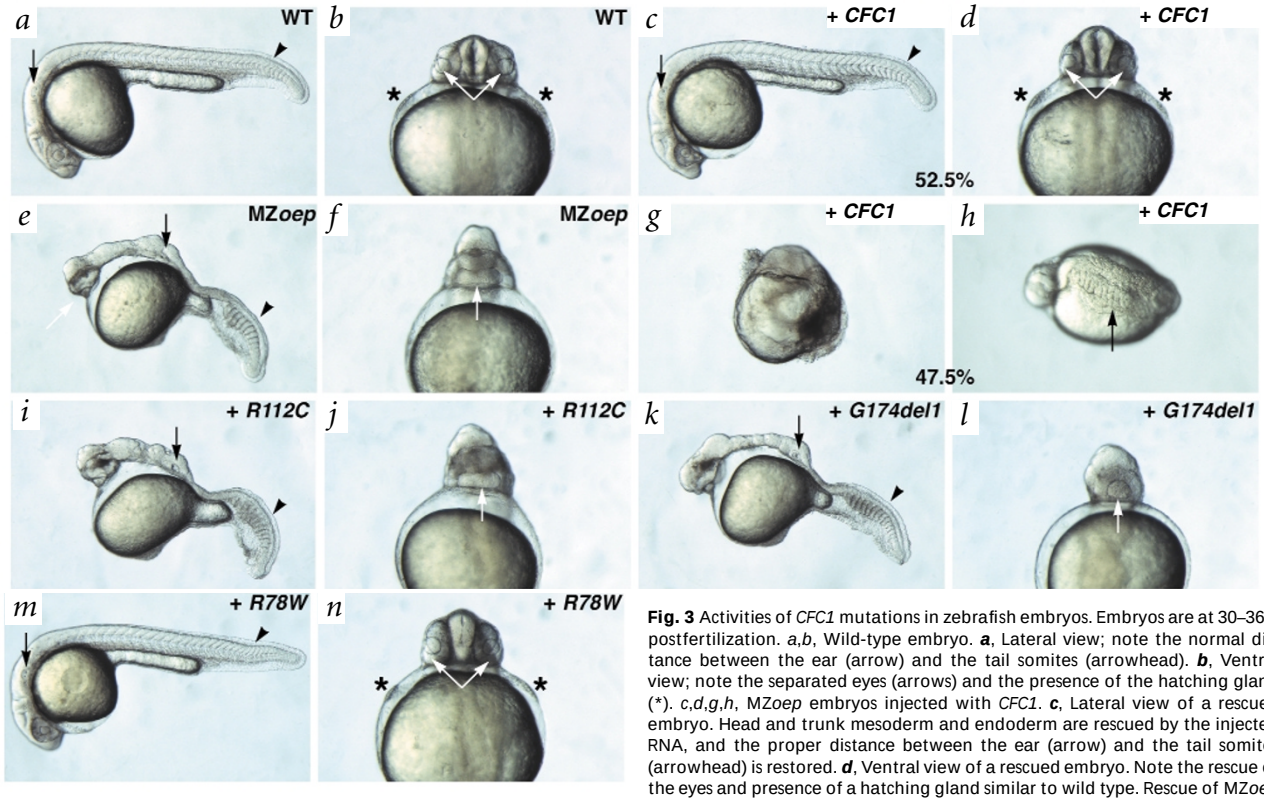

Fig. 3 Activities of *CFC1* mutations in zebrafish embryos. Embryos are at 30–36 h postfertilization. *a*,*b*, Wild-type embryo. ***a***, Lateral view; note the normal distance between the ear (arrow) and the tail somites (arrowhead). ***b***, Ventral view; note the separated eyes (arrows) and the presence of the hatching gland (*). *c*,*d*,*g*,*h*, MZ*oep* embryos injected with *CFC1*. ***c***, Lateral view of a rescued embryo. Head and trunk mesoderm and endoderm are rescued by the injected RNA, and the proper distance between the ear (arrow) and the tail somites (arrowhead) is restored. ***d***, Ventral view of a rescued embryo. Note the rescue of the eyes and presence of a hatching gland similar to wild type. Rescue of MZ*oep* mutant phenotypes was observed in 52.5% of injected embryos (74/141 with complete or partial rescue). ***g***,***h***, MZ*oep* embryos injected with *CFC1* display dominant phenotypes in 47.5% (67/141) of embryos. The embryo in (*g*) has no obvious anterior-posterior axis. The embryo in (*h*) is oriented with prospective anterior to the left. Note the trunk somites (arrow) indicating that trunk mesoderm is rescued in these embryos. Similar defects were observed on injection of *CFC1* into wild-type embryos. ***e***,***f***, MZ*oep* embryo. ***e***, Lateral view; head and trunk mesoderm and endoderm do not form. Note ear (arrow) and cyclopic eye (open arrow). The lack of the trunk results in a short distance between the ear (arrow) and the few tail somites that form (arrowhead). ***f***, Ventral view; only a cyclopic eye (arrow) forms and the hatching gland is absent. ***i***,***j***, Lateral and ventral view of an MZ*oep* embryo injected with R112C showing a lack of rescue (n=106). ***k***,***l***, Lateral and ventral views of an MZ*oep* embryo injected with G174del1 showing a lack of rescue (n=103). Arrows and arrowheads in (*i*,*j*,*k*,*l*) are as in (*e*,*f*). ***m***,***n***, Lateral and ventral views of an MZ*oep* embryo injected with R78W showing complete rescue in 51.9% (42/81) and partial rescue in 48.1% (38/81). No dominant phenotypes were observed with R78W. Arrows, arrowheads and * in (*c*,*d*,*m*,*n*) are like those in (*a*,*b*).

in exon 6. The deletion results in a frameshift that eliminates the membrane-associating domain and terminates 55 codons downstream of the deletion (Fig. 1*b*). Both affected individuals had dextrocardia and transposition of the great arteries, yet differed in their internal anomalies. Patient 2 had L-isomerism, whereas patient 3 had R-isomerism (Table 1). The 522delC mutation was also present in one of the phenotypically normal parents of patient 3. Previous studies (B.C., unpublished data) identified a missense mutation in *NODAL* in this patient, although the functional significance of this variation is unknown. In patient 4 with sporadic laterality defects (Table 1), a heterozygous 562C→T transition corresponding to R189C was seen in exon 6 on the carboxy side of the membrane-associating domain. This residue is not conserved among EGF-CFC family members and the function of the protein seemed normal in all of the assays used. In five unrelated sporadic patients of African American descent (Table 1, patients 5–9), a heterozygous 232C→T transition predicting an R78W change was detected just upstream of the EGF-domain in exon 3. This 232C→T nucleotide change was accompanied by a silent sequence variation predicting P75P as the haplotype [225C→A; 232C→T], suggesting a founder effect. Although this arginine residue is not conserved among EGF-CFC family members, it is flanked by conserved residues (Fig. 1*b*). This R78W change was not detected in over 300 chromosomes (based on a *Sma*I RFLP) from our control individuals of European descent, but was present in 4 of 136 chromosomes (3%) from African American control individuals. Given that this missense mutation leads to cellular localization and activity different from those of wild type, a more rigorous evaluation of the potential of this variant as a predisposing allele, specific to a subset of the African American population, needs to be performed.

Potential cellular localization differences of these four CRYPTIC variants were assessed by immunofluorescence staining of transfected COS-7 cells. Epitope-tagged CRYPTIC proteins were analysed in intact (Fig. 2*a*,*c*,*e*,*g*,*i*) and detergent-permeabilized (Fig. 2*b*,*d*,*f*,*h*,*j*) cells, transfected with the indicated haemagglutinin (HA)-tagged constructs. Unlike wild-type CRYPTIC, the G174del1 mutant is absent from the cell surface (Fig. 2*e*) and may instead be partially associated with extracellular matrix (Fig. 2, arrow). Additionally, G174del1 is detected in permeabilized cells (Fig. 2*f*), indicating that its absence from the cell surface is not the result of rapid intracellular degradation or lack of expression. The R112C and R78W mutants are localized to the cell surface, but display prominent clustering of staining (Fig. 2*c*,*g*, arrow) that is not found with wild-type (Fig. 2*a*) or R189C (Fig. 2*i*) proteins. The significance of the clustering pattern is currently unknown.

To test the *in vivo* activity of the *CFC1* variants described above, RNA transcripts (generated *in vitro*) corresponding to wild-type and variant CRYPTIC proteins were injected into zebrafish maternal-zygotic *oep* (MZ*oep*) mutant embryos at the 1–4-cell stage and then examined for rescue at 30–36 hours after fertilization[11] (Fig. 3). *CFC1* was able to rescue several aspects of the MZ*oep* mutant phenotype. Injected embryos developed two separated eyes, notochord, hatching gland, somites and other mesodermal derivatives (Fig. 3*c*,*d*). In contrast, the R112C and G174del1 mutants are completely inactive in rescuing the MZ*oep* mutant phenotype (Fig.

3*i–l*), establishing that these nucleotide changes abrogate the EGF-CFC activity of *CFC1*. In contrast, R78W (Fig. 3*m*,*n*) and R189C (data not shown) transcripts can rescue the phenotype. Unlike other EGF-CFC RNA transcripts, including mouse *Cfc1* (ref. 11, and J. Zhang, W.S. Talbot and A.F.S., unpublished data), wild-type *CFC1* induces dominant effects. We found that 50% of injected wild-type embryos were developmentally delayed or showed abnormalities during gastrulation (Fig. 3*g*,*h*). The major abnormalities resembled defects in epiboly, the gastrulation movement that leads to the enveloping of the yolk cell by the blastoderm[15,16]. This dominant phenotype was also seen with *CFC1* injected into MZ*oep* mutants. Moreover, R189C behaved identically to wild-type *CFC1* (data not shown). The observed phenotypes are not obviously related to the role of EGF-CFC factors in NODAL signalling (ref. 11). It is thus conceivable that in addition to its activity in NODAL signalling, CRYPTIC interacts with additional cellular factors, leading to the observed dominant (neomorphic) phenotypes. R78W had no dominant effect when injected into wild-type zebrafish and fully rescued most *oep* mutants (Fig. 3*m*,*n*). This result establishes that R78 in CRYPTIC is required to induce the observed dominant phenotypes, but is not essential for the role of CRYPTIC in NODAL signalling. The rescue assays indicate that R189C behaves like wild-type *CFC1*, whereas R112C and G174del1 inactivate *CFC1*. In contrast, the R78W mutant protein has rescuing ability, but lacks the dominant effect seen with the wild-type CRYPTIC protein.

The phenotypes observed in patients with *CFC1* mutations are consistent with heterotaxy, but are not completely concordant with the R-isomerism observed in *Cfc1*$^{-/-}$ mice[12,13]. The highly penetrant phenotype of these mice is believed to be a consequence of the absence of L-R asymmetric gene expression in the lateral plate mesoderm during embryogenesis, including *Leftb*, *Pitx2* and *Nodal* (refs 12,13). Similarly, zebrafish MZ*oep* mutants that have been partially rescued by *oep* mRNA injection also display heterotaxy with lack of asymmetric marker expression[18]. In contrast to humans with laterality defects, heterozygous *Cfc1* mice and *oep* fish are phenotypically wild type. The two laterality patients with the G174del1 mutation provide an interesting contrast: one presenting with right isomerism, the other one with left isomerism. A similar discrepancy has been observed in siblings presumably inheriting the same *ZIC3* mutation from their father with *situs inversus*[19].

Our mutational analysis of *CFC1* expands on the known zebrafish *oep* mutations tz57 (which changes the initiator ATG to GTG and predicts translation initiation 9 amino acids downstream) and m134 (S168X resulting in a truncation of the C terminus; ref. 10). The effect of the latter mutation is similar to that seen with the human G174del1 with respect to abrogation of cell-surface association (Fig. 2*e*), shown to be essential for wild-type oep function[10], and now for CRYPTIC function as well. The R112C mutation in *CFC1* leads to complete loss of function, as well as an abnormal cell surface distribution, demonstrating that the EGF domain is required for CRYPTIC function. The human protein contains an additional residue (R78) that is not present in the EGF-CFC proteins Oep, Cripto and FRL-1 (Fig. 1). It is noteworthy that the human R78W variation results in an altered cell-surface distribution (Fig. 2*g*) and lacks the dominant phenotypic effect seen with wild-type CRYPTIC or R189C. Because these dominant phenotypes are not found on expression of other EGF-CFC genes (ref. 11 and J. Zhang, W.S. Talbot & A.F.S., unpublished data), it is conceivable that, in addition to its role in NODAL signalling, CRYPTIC might have extra functions that are mediated by the region encompassing R78W.

The phenotypic distinctions between humans with heterozygous *CFC1* loss-of-function mutations and *Cfc1*$^{-/-}$ mice might reflect differences in gene dosage combined with environmental and/or genetic modifier effects that contribute to these differences. Because high-level *Nodal* expression in the lateral plate mesoderm is dependent on amplification through a positive feedback loop[17,20], Nodal signalling may be particularly sensitive to gene dosage effects for either *Nodal* itself[21,22] or its co-factor *Cfc1*. Consequently, humans with heterozygous *CFC1* mutations may be sensitized to additional perturbations in the L-R pathway, perhaps leading to difficulties in establishing or maintaining the NODAL amplification loop. Therefore, we propose that decreased CRYPTIC activity in combination with other factors may result in altered levels of NODAL signalling in the lateral plate mesoderm, leading to stochastic or incomplete specification of 'leftness' followed by heterotaxic morphogenesis.

Methods

BAC isolation and sequencing. To isolate a *CFC1* genomic clone, a BAC library was screened with a primer pair (5′–CGGCCGCGCTGCT GCAGGAAC–3′ and 5′–AGCGGTCAGGCGTCTGGAGGG–3′) based on the EST AA862263 and a single clone, 268p16 (Genome Systems), was isolated for further analysis. A 10-kb *Eco*RI fragment containing full-length *CFC1* was subcloned from 268p16 into pBlue-Script and was sequenced in its entirety. Because of the G/C-rich nature of the amplicon, PCR proved successful only when using PCR$_X$ Enhancer System (Life Technologies). A 2× concentration of enhancer solution and recommended concentrations of other kit components were used; reactions were run at an annealing temperature of 55 °C for 35 cycles. A single BAC clone was isolated that corresponded to the Genome Systems address 268p16. Southern-blot analysis of 268p16 demonstrated that a single, 10-kb *Eco*RI fragment hybridized to the above amplicon when used as a probe. The 10-kb fragment was subcloned into pBlue-Script and automated sequencing (ABI^{377}) was initiated using forward and reverse primers based on existing ESTs (AA862263, N68345 and AA528135). To complete sequencing, additional primers were designed from 5′ and/or 3′ ends of newly generated sequence. The final exon/intron boundaries were determined with successful cDNA isolation.

cDNA cloning. For isolation of *CFC1* cDNA sequences, a human ovary 5′-STRETCH cDNA library (Clontech) was plated and screened with a 3′ *CFC1* probe and a single clone was isolated that consisted of exons 4, 5 and 6 and demonstrated high homology to the EST. To determine the remaining 5′ exons, 5′ RACE (Life Technologies) was carried out using human fetal brain total RNA (Clontech); procedures followed the manufacturer's recommendations using 3′ gene-specific primers (GSP) and provided 5′ primers, but all PCR steps used the PCR$_X$ Enhancer System with 1× enhancer solution. The GSPs included the following: GSP1, 5′–AGCG GTCAGGCGTCTGGAGGG–3′ used for RT; GSP2, 5′–TGCGCCTCTG GTCATGCTCGC–3′ used for primary PCR with an annealing temperature of 58 °C; and GSP3, 5′–CGCAGAAGCTGCCCAGCAC–3′ used for secondary PCR with an annealing temperature of 58 °C. On the basis of RACE product sequences, a full-length coding sequence (CDS) was PCR amplified from fetal brain cDNA using primers 5′–GATCGGATCCTCTTCAAT GCACTAAGAGAAGGAG–3′ and 5′–GATCGGATCCTTCA GCTTACG GTAAACTAAACAC–3′ with 1× PCR$_X$ enhancer. Nested *Bam*HI sites are underlined and the amplicon represents *CFC1* nt 353–1,111.

Mutational screening. Patient DNA was prepared by standard methods from human blood and/or lymphoblastoid cell lines and was analysed according to IRB guidelines of the DIR NHGRI. SSCP analysis was carried out using intronic and/or UTR-based PCR primers that flanked the *CFC1* exons. Primer design and PCR conditions followed the Oligos 4.0 program; annealing temperatures and PCR$_X$ enhancer concentrations were included with exon primer pairs (exon 1, 5′–CTGGAGTAAAGACAC CTTCAAATG–3′ and 5′–ATTTATTCTGAGGCTCTTAAGACC–3′, 50 °C with 0.5× enhancer; exon 2/3, 5′–GATGTAAATTTCTGCTTATACTTC–3′ and 5′–TGAATTTATCCTACATATTCTCAG–3′, 50 °C with 0.5× enhancer; exon 4, 5′–AGCAAACAACTTG GCTGGAG–3′ and 5′–CAGACC CGCAGGTCCCTCAC–3′, 55 °C with 2× enhancer; exon 5, 5′–CCACCG CATTGATGCAGGTC–3′ and 5′–GCACTGTGGATCGGTATGGAGG–3′, 55 °C with 2× enhancer; exon 6, 5′–TATTGCACTCTCTCAAACCGAG–3′ and 5′–TGTCCCTCTCCCAAGGATCTG–3′, 54 °C with 1× enhancer). PCR reactions were run at 10 µl with 1 µCi of α-^{32}P-dCTP and all samples were

resolved on 0.5× non-denaturing MDE gels (FMC BioProducts) overnight between 4–6 Watts at 25 °C, except exon 2/3, which was run at 8 Watts at 25 °C or 4 °C. In addition to mutations in *CFC1*, the following changes likely to represent single-nucleotide polymorphisms were identified: N21H (61A→C), R47Q (140G→A) and P75P (225C→A; seen in isolation once, but more commonly as [225C→A; 232C→T] in conjunction with R78W). Also, we detected A145T (433G→A), P196P (588C→A), L220L (606G→C) and P204P (612C→A); intervening sequence variations in intron 3, IVS-4G>→T and IVS-81G→A; and the haplotype P196P;R200R;L202L, denoted [588C→A;599G→T;606G→C], in one laterality patient.

Site-directed mutagenesis and construct design. Generation of *CFC1* cDNA mutants used the Transformer Site-Directed Mutagenesis kit (Clontech) and followed the manufacturer's recommendations. Standard recombinant DNA techniques were used to build wild-type and haemagglutinin-tagged (HA) *CFC1* in the vector pCR2.1 (Invitrogen) with the epitope tag inserted between residues 25 and 26 following the signal sequence. For transfection experiments, the site-directed mutagenesis constructs were re-cloned into the expression vector pEFneo. For the production of synthetic RNA for injection experiments, the constructs were re-cloned into pSP64 poly(A) (Promega). Details on construct design are available on request.

Immunofluorescence analysis of transfected cells. COS-7 cells grown on poly-L-Lysine coated coverslips were transfected using Lipofectamine reagent in serum-free OPTI-MEM medium (Life Technologies), followed by incubation in DMEM containing 10% fetal bovine serum. Cells were grown for 24 h, and then fixed in 4% paraformaldehyde for 15 min. Control slides were permeabilized by treatment with 1% Triton X-100 for 5 min. Immunofluorescence detection of HA-tagged CRYPTIC proteins was performed using HA-monoclonal antibody (Covance) and FITC-conjugated anti-mouse IgG secondary antibody (Jackson Immunoresearch), followed by counterstaining with DAPI to visualize nuclei.

Functional complementation in zebrafish embryos. Plasmids were linearized with *Eco*RI and sense strand mRNA was synthesized using the SP6 Message Machine kit (Ambion). RNA was injected at 50 pg/embryo as described[11].

GenBank accession numbers. Human *CFC1* cDNA, AF312769, human *CFC1* genomic sequence, AF312925.

Acknowledgements

We thank the patients and their families for participation. R.D.B. is supported by a postdoctoral fellowship from the Damon Runyon-Walter Winchell Cancer Research Fund. A.F.S. is a Scholar of the McKnight Endowment Fund for Neuroscience. The authors are supported by grants from the NIH (B.C., A.F.S. and M.M.S.), the US Army Breast Cancer Research Program (M.M.S.) and the Division of Intramural Research, National Human Genome Research Institute, NIH (M.M.).

Received 24 August; accepted 25 September 2000.

1. Kosaki, K. & Casey, B. Genetics of human left-right axis malformations. *Cell Dev. Biol.* **9**, 89–99 (1998).
2. Capdevila, J., Vogan, K.J., Tabin, C. & Izpisua Belmonte, J.C. Mechanisms of left-right determination in vertebrates. *Cell* **101**, 9–21 (2000).
3. Burdine, R. & Schier, A.F. Conserved and divergent mechanisms in left-right axis formation. *Genes Dev.* **14**, 763–776 (2000).
4. Schier, A.F. & Shen, M.M. Nodal signalling in vertebrate development. *Nature* **403**, 385–389 (2000).
5. Gebbia, M. *et al*. X-linked *situs* abnormalities result from mutations in *ZIC3*. *Nature Genet.* **17**, 305–308 (1997).
6. Kosaki, K. *et al*. Characterization and mutation analysis of human LEFTYA and LEFTYB, homologues of murine genes implicated in left-right axis development. *Am. J. Hum. Genet.* **64**, 712–721 (1999).
7. Kosaki, R. *et al*. Left-right axis malformations associated with mutations in *ACVR2B*, the gene for human activin receptor type IIB. *Am. J. Med. Genet.* **82**, 70–76 (1999).
8. Shen, M.M. & Schier, A.F. The EGF-CFC gene family in vertebrate development. *Trends Genet.* **16**, 303–309 (2000).
9. Shen, M.M., Wang, H. & Leder, P. A differential display strategy identifies Cryptic, a novel EGF-related gene expressed in the axial and lateral mesoderm during mouse gastrulation. *Development* **124**, 429–442 (1997).
10. Zhang, J., Talbot, W.S. & Schier, A.F. Positional cloning identifies zebrafish one-eyed pinhead as a permissive EGF-related ligand required during gastrulation. *Cell* **92**, 241–251 (1998).
11. Gritsman, K. *et al*. The EGF-CFC protein one-eyed pinhead is essential for nodal signaling. *Cell* **97**, 121–137 (1999).
12. Gaio, U. *et al*. A role of the cryptic gene in the correct establishment of the left-right axis. *Curr. Biol.* **9**, 1339–1342 (1999).
13. Yan, Y.-T. *et al*. Conserved requirement for EGF-CFC genes in vertebrate left-right axis formation. *Genes Dev.* **13**, 2527–2537 (1999).
14. Minchiotti, G. *et al*. Membrane-anchorage of Cripto protein by glycosylphosphatidylinositol and its distribution during early mouse development. *Mech. Dev.* **90**, 133–142 (2000).
15. Kane, D.A. *et al*. The zebrafish epiboly mutants. *Development* **123**, 47–55 (1996).
16. Solnica-Krezel, L. *et al*. Mutations affecting cell fates and cellular rearrangements during gastrulation in zebrafish. *Development* **123**, 67–80 (1996).
17. Osada, S.I. *et al*. Activin/nodal responsiveness and asymmetric expression of a Xenopus nodal-related gene converge on a FAST-regulated module in intron 1. *Development* **127**, 2503–2514 (2000).
18. Meno, C. *et al*. Mouse lefty2 and zebrafish antivin are feedback inhibitors of nodal signaling during vertebrate gastrulation. *Mol. Cell* **4**, 287–298 (1999).
19. Niikawa, N., Kohsaka, S., Mizumoto, M., Hamada, I. & Kajii, T. Familial clustering of situs inversus totalis, and asplenia and polysplenia syndromes. *Am. J. Med. Genet.* **16**, 43–47 (1983).
20. Saijoh, Y. *et al*. Left-right asymmetric expression of lefty2 and nodal is induced by a signaling pathway that includes the transcription factor FAST2. *Mol. Cell* **5**, 35–47 (2000).
21. Collignon, D.B., Varlet, I. & Robertson, E. Relationship between asymmetric nodal expression and the direction of embryonic turning. *Nature* **381**, 155–158 (1996).
22. Nomura, M. & Li, E. Smad2 role in mesoderm formation, left-right patterning and craniofacial development. *Nature* **393**, 786–790 (1998).